21AM1D-03

Frequency Control of Transmission Property for Multiband Frequency Selective Surfaces

Kunio Sakakibara [#1], Katsuyuki Tachikawa [#2], Yuto Amano [#3], Kiyotaka Kumaki [*4],
Satoshi Hori [*5], Nobuyoshi Kikuma [#6], Hiroshi Hirayama [#7]

[#] *Department of Computer Science and Engineering, Nagoya Institute of Technology*
Gokiso-cho, Showa-ku, Nagoya 466-8555, Japan
[1,2,3] sakaki@nitech.ac.jp
[6] kikuma@m.ieice.org
[7] hirayama@nitech.ac.jp

[*] *KOJIMA PRESS INDUSTRY CO., LTD*
15, Hirokuden, Ukigai-cho, Miyoshi-shi, Aichi-ken, 470-0207, Japan
[4] kumaki@kojima-tns.co.jp
[5] hori@kojima-tns.co.jp

***Abstract*—Multiband frequency selective surfaces are developed in this work. Not only multiple loops but also a single meander loop can generate multiple transmission frequencies. The transmission frequencies can be controlled by the dimensions of the geometry. The frequency dependencies of transmission and stop characteristics are evaluated by electromagnetic simulations and measurements using a developed measurement system.**

I. Introduction

Lightweight and recyclable plastic cars are attractive in cheap to run and extremely fuel efficient. On the other hand, many wireless systems are being equipped or used in cars, such as mobile phone, WiFi, digital TV, radio, ETC (Electronic Toll Collection System), GPS (Global Positioning System), smart key systems, etc. Furthermore, electromagnetic noise is significantly increasing with growth of electric and hybrid vehicles. However, electromagnetic shielding capability in plastic is much less than metal and glass. The electromagnetic interference between the systems and the electromagnetic noises from large currents flowing in wire harnesses affect to the system performance.

FSS (Frequency Selective Surface) [1], [2] could be one of the solutions to protect the electronics systems in cars from interferences and electromagnetic noises, serving wireless systems in passenger's cars simultaneously. Multiband FSSs for transmission property at some specific frequencies are developed in this work. A periodic loop slot performs bandpass FSS characteristics. Therefore, multiple loop slots perform multiple bandpass characteristics [3]. A periodic single meander (fractal) loop slot is also designed to be multiple frequencies [4]. Furthermore, the size of the period becomes small in the meander loop slot, which is advantageous when the physical area for FSS is too small to achieve periodic feature. The performances of the developed FSSs are evaluated by electromagnetic simulations and measurements of the developed measurement system.

II. Periodic Structures of FSS

Five different periodic structures are developed for FSSs to investigate dual transmission band properties and size reduction. Figure 1 shows metal patterns of a period printed on the Polycarbonate board (ε_r=2.9). Figure 1(a) is a fundamental single square loop (SSL) slot FSS which performs a transmission property when the loop length equals one wavelength. Therefore, the resonant frequency is expressed by

$$f_0 = \frac{c}{\lambda\sqrt{\varepsilon_r}} = \frac{c}{4(a-w)\sqrt{\varepsilon_r}},$$

where c is light speed, a is one outer side length of the square loop slot and w is slot width. The resonant frequency can be controlled by these dimensions.

Based on the FSS (a), four dual-band FSSs of double square loop (DSL) (b), multi periodicity combined loop (MPCL) (c), fractal loop (d), and multi periodicity combine fractal loop (MPCFL) (e)

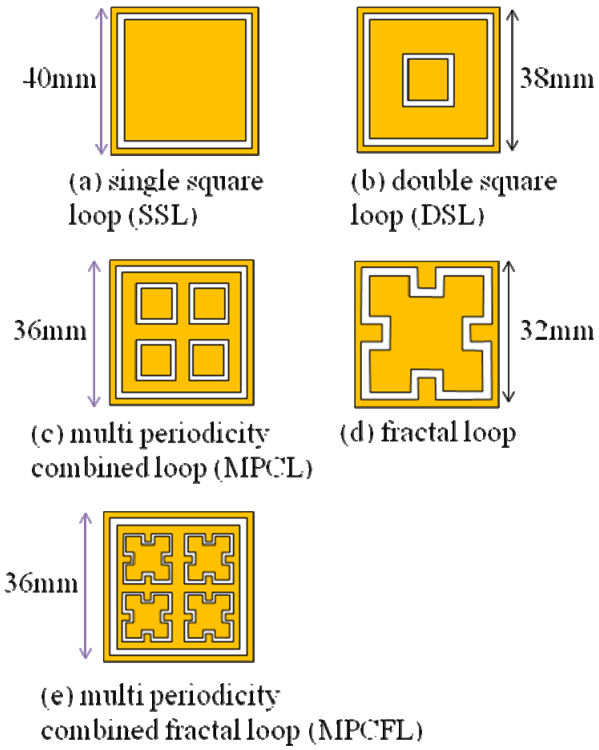

Fig. 1 Periodic structures for FSS.

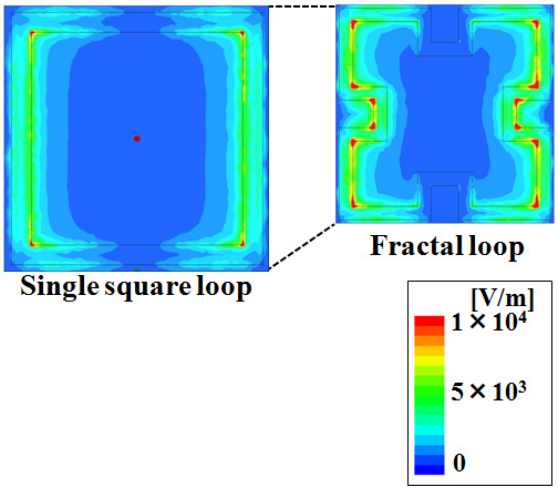

Fig. 2 Electric field distributions of FSSs with SSL and Fractal loop at 1.5 GHz.

are designed. As for the FSSs (b), (c), the outer loop creates a lower resonant frequency and the inner loops are for a higher resonant frequency [3]. Four smaller loops are arranged in the outer loop of the FSS (c) for broad bandwidth. The size of the period is gradually smaller from FSS (a) to (c). It could be caused by increasing mutual coupling between loops. Regarding the FSS (d) with meander path, overall length of the loop is almost one wavelength

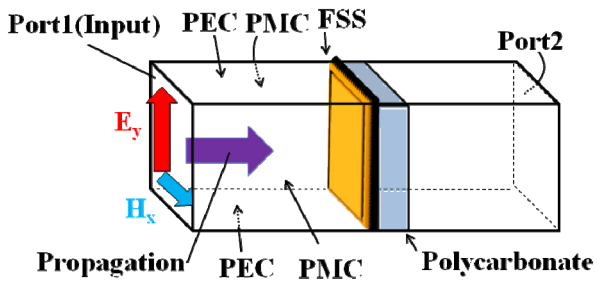

Fig. 3 Analysis model with periodic boundary condition.

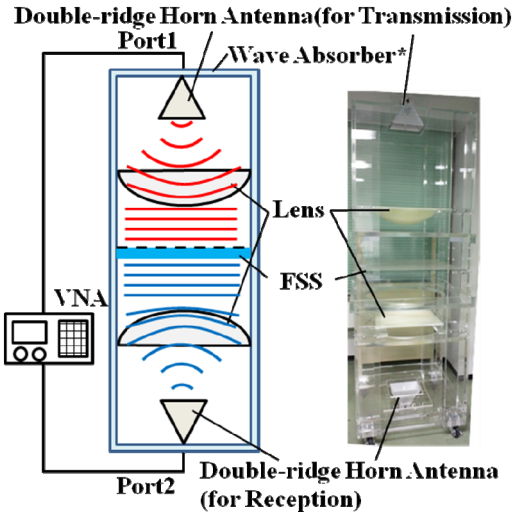

Fig. 4 Measurement setup of scattering parameters for FSSs

as well as other FSSs. Figure 2 shows electric field distribution on the metal plane. Strong electric field bends along the meander slot. Consequently, dual resonance is achieved and the period of the FSS can be smaller than the other FSSs, simultaneously [5].

III. Simulation and Measurement

The periodic structures are effectively analysed by assuming Floquet's periodic boundary condition in the electromagnetic simulations. Figure 3 shows the analysis model of the periodic structures. Perfect electric conductor (PEC) and perfect magnetic conductor (PMC) surround around the analysis area for boundary condition between the periods. On the PEC, tangential component of the electric field equals to zero. On the other hand on the PMC, tangential component of the magnetic field equals to zero. Therefore, the analytical model simulates periodic condition when *y*-polarized plane

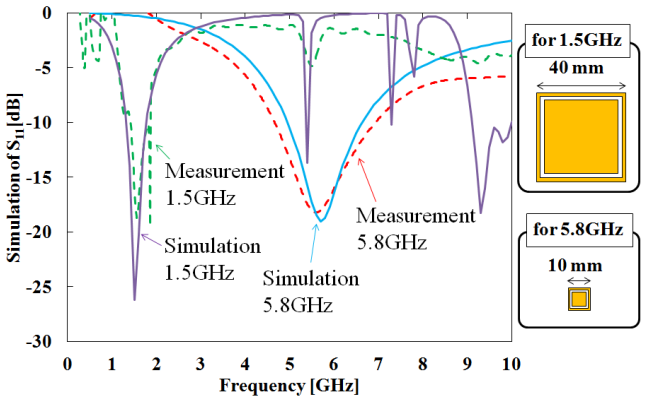

Fig. 5 Scattering parameters of fundamental loop slot FSS.

wave input toward –z direction normal to FSS. Ansys HFSS is used in the simulations.

Figure 4 shows the developed measurement system for scattering parameters of planar sheets. The size of the acrylic frame is 2300mm height x 810mm depth x 810mm width. The spherical wave radiated from the double-ridge horn antenna fed by the vector network analyser is transferred to the plane wave by the dielectric lens. The plane wave is scattered by a FSS under test. Reflection and transmission waves are transferred again to the spherical wave by the lenses and are received by the same and the other horn antennas, respectively. The fabricated FSS is printed on 500mm-square Polycarbonate board by silk-screen printing, and set at the middle of the measurement setup horizontally. To reduce the effect of circumference, the acrylic frame is surrounded by wave absorbers during measurement.

Figure 5 shows the simulated and measured S_{11} of the SSL (a) for 1.5GHz or 5.8GHz. As for the FSS of 1.5GHz, the measured data are disturbed in contrast to the simulation. It could be caused by the effect for the limited size of the fabricated FSS. However, resonances are observed and measured resonant frequencies agree well with the simulated ones in both designs of 1.5 and 5.8 GHz. Simulation validity is confirmed by the measurements.

Figure 6 shows the simulated comparison of S_{11} for dual-band FSSs (b), (c), (d) at both 1.5GHz and 5.8GHz. Broad bandwidth is observed at the higher resonant frequency (5.8GHz-band) by using FSS (c) because four loops are arranged closely.

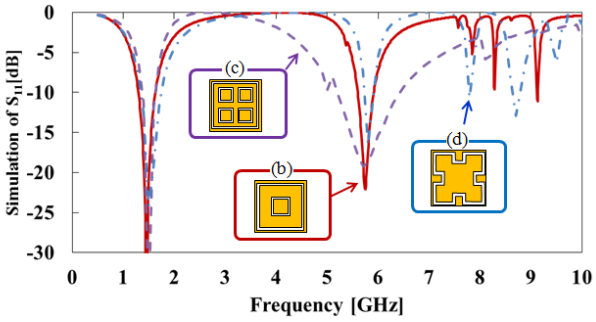

Fig. 6 Simulated comparison of S_{11} for FSS (b), (c), and (d)

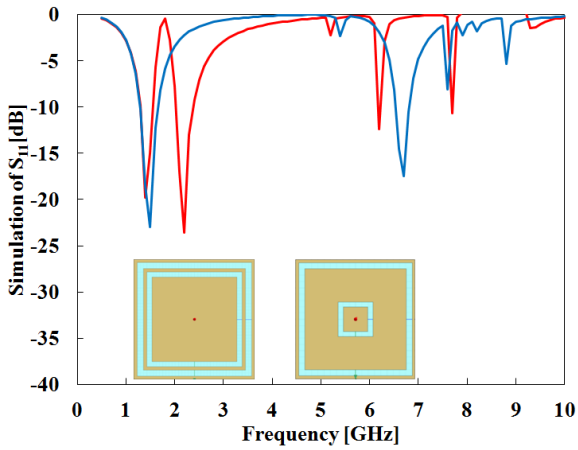

Fig. 7 Simulated reflection characteristics of double square loop FSS changing size of the inner loop.

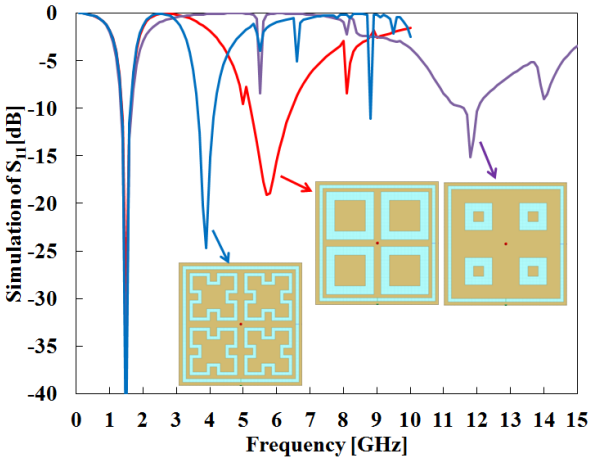

Fig. 8 Control range of resonant frequency using multi periodicity combined loop FSS.

Figure 7 shows the reflection characteristics when the size of the inner slot of DSL (b) changes. When the size of the inner slot increases, the resonant frequency shifts lower close to the

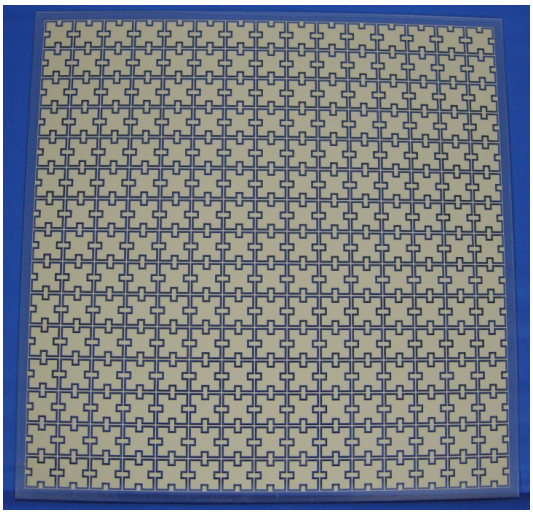

Fig. 9 Photograph of the fractal loop FSS.

resonant frequency of the outer slot. On the other hand of MPCL (c), the maximum size of the inner slot is limited to be a quarter of DSL. Therefore, the lowest resonant frequency of the inner slot is 5.7 GHz as shown in Fig. 8, although the bandwidth is wider than DSL. However, when fractal slots are used for inner slots, the higher resonant frequency can drop to 3.9 GHz.

The performance of the developed FSS is confirmed by experiments. The photograph of the fabricated FSS is shown in Fig. 9. 15 x 15 periods are arranged on the 500mm x 500mm plate. Figures 10 and 11 show the measured S_{11} of FSSs (c) and (d), respectively. Broad bandwidth at the higher resonant frequency in FSS (c) and small period in FSS (d) are confirmed by the simulations and the measurements. All FSSs perform transparent property at the design frequencies.

IV. Conclusion

Dual-band FSSs on plastic board that transmit 1.5GHz and 5.8GHz are developed and are evaluated by HFSS analysis and measurement. As for the close arrangement of inner elements in FSS (c), broad bandwidth is observed at higher resonant frequency than the other FSSs. The period of the FSS can be smaller by using fractal structure. Measurement system is developed and its validity is confirmed by comparison of simulation with measurement. The bandwidth and resonant frequencies of FSS are confirmed by the system.

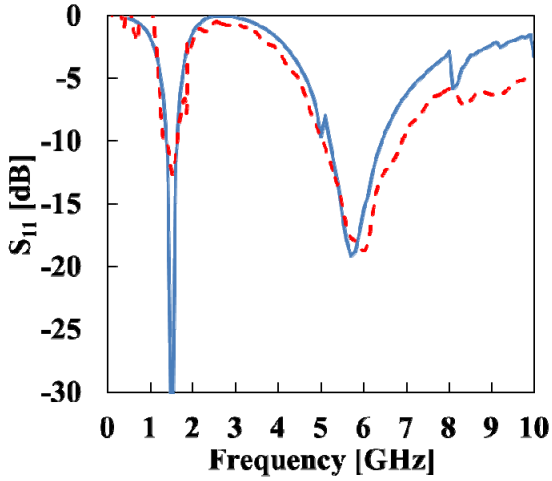

Fig. 10 Simulated and measured reflection characteristics of multi periodicity combined loop FSS (c).

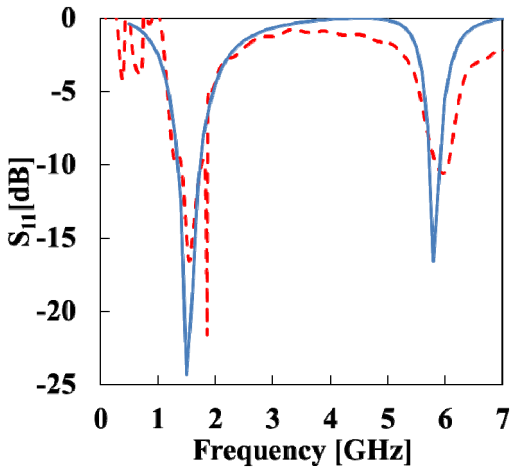

Fig. 11 Simulated and measured reflection characteristics of fractal loop FSS (d).

References

[1] B. A. Munk, Frequency Selective Surfaces: Theory and Design, Wiley-Interscience, 2000.

[2] F. Bayatpur, Metamaterial-Inspired Frequency-Selective Surfaces: Proquest, Umi Dissertation Publishing, 2011.

[3] J. P. Gianvittorio, J.Romeu, S. Blanch, and Y. Rahmat-Samii,"Self-Similar Prefractal Frequency Selective Surfaces for Multiband and Dual-Polarized Applications" IEEE Trans. Antennas and Propagation, vol.51, no.11, pp.1798-1803 Nov. 2003.

[4] K. Tachikawa, K. Sakakibara, N. Kikuma, H. Hirayama, K. Kumaki, S. Hori, "Transmission properties of dual-band loop slot Frequency Selective Surfaces on plastic board," 2012 15th International Symposium on Antenna Technology and Applied Electromagnetics (ANTEM), pp. 1-4, June 2012, Toulouse, France.

[5] H. L. Liu, K. L. Ford, and R. J. Langley, "Design Methodology for a Miniaturized Frequency Selective Surface Using Lumped Reactive Components" IEEE Trans. Antennas and Propagation, vol.57, no.9, pp.1239-1245,Sep. 2009.